UC Davis

UC Davis Previously Published Works

Title

Advanced monitoring of almond orchard water status using machine learning and remote sensing

Permalink

https://escholarship.org/uc/item/3g27d7s7

Journal

Scientia Horticulturae, 342

ISSN

0304-4238

Authors

Peddinti, Srinivasa Rao

Kisekka, Isaya

Publication Date

2025-02-01

DOI

10.1016/j.scienta.2025.114020

Copyright Information

This work is made available under the terms of a Creative Commons Attribution License, available at https://creativecommons.org/licenses/by/4.0/

Peer reviewed

eScholarship.org Powered by the California Digital Library
University of California

Scientia Horticulturae 342 (2025) 114020

Contents lists available at ScienceDirect

Scientia Horticulturae

journal homepage: www.elsevier.com/locate/scihorti

Research Paper

Advanced monitoring of almond orchard water status using machine learning and remote sensing

Srinivasa Rao Peddinti [a], Isaya Kisekka [a,b,*]

[a] Department of Land, Air & Water Resources, University of California Davis, Davis, CA, 95616, USA
[b] Department of Biological and Agricultural Engineering, University of California Davis, Davis, CA, 95616, USA

ARTICLE INFO

Keywords:
Stem water potential
Random forest
Precision agriculture
Irrigation
Water management

ABSTRACT

Water management is essential for optimizing yields in almond orchards, particularly in regions with limited water resources. This work integrates different sources of information (satellite imagery, meteorological data, soil data, and machine learning techniques) to monitor and predict the spatial variability of stem water potential (SWP) in an almond orchard. A random forest (RF) model was developed using weekly SWP measurements collected between 2019 and 2021 at 24 monitoring locations. Predictor variables included meteorological variables (air temperature, solar radiation, wind speed, relative humidity, vapor pressure deficit), soil parameters (soil bulk density and soil water content), and vegetation indices derived from satellite imagery (normalized difference vegetation index) and the evaporation fraction were used. The RF model demonstrated high accuracy in predicting SWP, with a Nash-Sutcliffe Efficiency (NSE) of 0.91 and a root mean square error (RMSE) of 0.17 MPa, as evidenced by the goodness-of-fit evaluation. The cumulative probability plot indicated that 78.2 % of the NSE values fall within the "very good" range and 21.8 % within the "good" range, underscoring the model's reliability. It was found that the key variables for SWP prediction are air temperature, evaporation fraction, wind speed, and solar radiation. Spatial maps generated with high-resolution aerial imagery by the model revealed significant within-field variability, particularly during critical growth stages such as the hull split period in July. During this period, the orchard was managed using deficit irrigation strategies, a common practice to mitigate hull rot and optimize water use, which resulted in lower (more negative) SWP values indicating water stress. These maps highlighted areas of the orchard experiencing greater water stress, guiding more precise irrigation management. This study highlights the importance of integrating high-resolution remote sensing data with machine learning algorithms to enhance water management practices in almond orchards. The findings suggest that the spatial and temporal predictions of SWP using the RF model can support precise irrigation scheduling, leading to improved water use efficiency and sustainability in almond production.

1. Introduction

Water scarcity is a critical issue in California, driven in part by the high water demands of almond cultivation. Almond orchards require approximately 900 −1350 mm of water annually (Goldhamer and Ferees, 2017), equating to 9000–13,500 m^3/ha, among the highest water demands for major crops in the region. This substantial water use, combined with frequent drought conditions and competing water demands for urban and environmental needs, underscores the pressure on California's limited water resources. These challenges necessitate a focus on improving irrigation efficiency and sustainable water management practices (Fulton et al., 2019; Parker et al., 2021). Almond is a high relevant/significant/key crop in California, contributing billions of dollars to the state's economy and supporting thousands of jobs. The state's Mediterranean climate, with its warm, dry summers and mild, wet winters, is ideal for almond cultivation. However, this same climate also poses significant challenges for water resource management. California's almond industry has grown exponentially over the past few decades, driven by high global demand for almonds. This growth has put immense pressure on the state's water resources, particularly during drought. Effective water management practices are essential to maximizing yield and ensuring sustainable almond

* Corresponding author at: Department of Land Air & Water Resources, and Department of Biological and Agricultural Engineering University of California Davis, Davis, One Shields Avenue, CA 95616-5270, USA.
E-mail address: ikisekka@ucdavis.edu (I. Kisekka).

https://doi.org/10.1016/j.scienta.2025.114020
Received 14 October 2024; Received in revised form 10 February 2025; Accepted 11 February 2025
Available online 18 February 2025
0304-4238/© 2025 The Authors. Published by Elsevier B.V. This is an open access article under the CC BY license (http://creativecommons.org/licenses/by/4.0/).

production (García-Tejero et al., 2020; Gutiérrez-Gordillo et al., 2020; Lipan et al., 2020). Despite the significance of traditional irrigation management practices such as monitoring evapotranspiration (ET), soil moisture, and plant physiological responses, these methods often fail to account for variability in crop type, cultivar, and climatic conditions (Bellvert et al., 2018; Drechsler et al., 2022). ET, which quantifies water loss through soil evaporation and plant transpiration, is fundamental to irrigation management (Peddinti and Kambhammettu, 2019). ET has been extensively studied (Calera et al., 2017; Fisher et al., 2017; Gowda et al., 2008; Xu and Singh, 1998) as a key component in understanding water balance and managing irrigation efficiently. Methods to measure ET range from simple pan evaporation techniques to complex remote sensing models. Each method has advantages and limitations, influencing its applicability in different contexts. A crucial measurement to assess the crop water status is the midday stem water potential (SWP) which is highly correlated with the plant stress responses and climatic conditions making it an invaluable tool for managing irrigation in nut and fruit crops (Shackel et al., 2021; Zhao et al., 2017b). However, measuring SWP is labor-intensive and time-consuming, requiring more time per sample (Zhao et al., 2017b). Various methods to automate and streamline SWP measurement are under investigation, yet manual methods remain the standard due to their accuracy. SWP is a critical indicator of plant water status, reflecting the tension or pressure within the plant's xylem tissues where water is transported from roots to leaves (Blum, 2011; Peiris et al., 2025). This measurement is particularly important in nut crops, such as almond orchards, to ensure optimal irrigation practices and to avoid water stress that can negatively impact crop yield and quality (Goldhamer et al., 2006; Kisekka, 2023). SWP is influenced by various factors, including soil moisture, atmospheric conditions, and the plant's physiological status (Choné et al., 2001; Lambers and Oliveira, 2019).

Advances in site-specific irrigation management have shown promise in improving water productivity by accounting for spatial soil variability (Hedley and Yule, 2009; O'Shaughnessy et al., 2015). Site-specific management customizes irrigation schedules and amounts to meet the needs of specific field zones, enhancing water use efficiency and crop yields. However, implementing these techniques requires detailed soil and crop data, which can be challenging to obtain and interpret. Accurate and timely detection of crop water stress is essential for optimal irrigation scheduling, but traditional methods often detect stress only after it has reached critical levels. Various approaches, including soil moisture sensors (Soulis et al., 2015), soil water balance methods (Pereira et al., 2020), plant-based measurements (Datta et al., 2018; Domínguez-Niño et al., 2020; Peddinti et al., 2020), and remote sensing technologies (Egea et al., 2010, 2009), have been developed to address this challenge. Soil moisture sensors, for instance, provide real-time data on soil water content, enabling precise irrigation decisions (Seyar and Ahamed, 2024). However, their effectiveness can be limited by soil heterogeneity and sensor placement (Sharma et al., 2021). Remote sensing techniques, particularly those using infrared thermometry and spectral vegetation indices, have gained attention for their potential to monitor crop water status over large areas. With the availability of extensive remote sensing data, researchers have increasingly explored its use in estimating plant water stress (Ma et al., 2018; Matese et al., 2018; Peddinti and Kisekka, 2022). These techniques allow for continuous monitoring over large areas, providing valuable insights into spatial water use and stress patterns. However, access to the information provided by this type of sensors is not always easy or timely. Thus, the use of remote sensors by means of drones requires a significant cost either in the acquisition of equipment or in access to the service through third parties. Additionally, access to information from satellites is limited by the time of monitoring and the atmospheric conditions existing during image capture, in addition to having a low resolution.

Recent studies have combined multispectral and thermal imagery with meteorological data to predict SWP, but there is a gap in research specifically integrating these data types with soil and vegetation indices using Random Forest (RF) models for almond orchards (Lin et al., 2020; Yang et al., 2022). The challenge lies in the heterogeneity of almond orchards, where soil properties, crop varieties, and microclimates can vary significantly. This variability complicates the development of accurate and reliable predictive models. However, these satellites cannot provide extremely fine spatial resolution. Although the WorldView-2 satellite has demonstrated its ability to estimate SWP over pear orchards at higher resolutions (Van Beek et al., 2013), the high cost and small swath size limit its practicality for larger areas. Using aerial or unmanned aerial vehicles (UAVs) instead of satellites allows for mapping with extremely high spatial and temporal resolution (Peddinti and Kisekka, 2022). UAVs can capture detailed images of small areas, providing high-resolution data that can be used to assess crop health and water status more accurately. Furthermore, UAVs have recently been used to monitor plant water status (Awais et al., 2023) and manage irrigation (Romero et al., 2018; Valente et al., 2022). UAV-based remote sensing platforms can be equipped with various sensors to measure reflectance, temperature, and other indicators of plant water status. This technology allows for more frequent and detailed monitoring than traditional methods, enabling more responsive and precise irrigation management. Machine learning algorithms (Gutiérrez et al., 2018; Lin et al., 2020; Martí et al., 2013; Poblete et al., 2017) are now being applied in various agricultural applications, including precision agriculture. These algorithms can process large datasets and identify patterns not immediately apparent to human observers. In irrigation management, machine learning models can analyze data from multiple sources, such as soil sensors, weather stations, and remote sensing platforms, to accurately predict crop water needs. RF models, in particular, have shown promise in predicting agricultural outcomes (Badshah et al., 2024; Rashid et al., 2021) due to their ability to handle large datasets with many variables and their robustness against overfitting. RF models use an ensemble of decision trees to improve prediction accuracy and can manage nonlinear relationships and interactions between variables (Auret and Aldrich, 2012; Rodriguez-Galiano et al., 2015). In this study, the RF model incorporated diverse data types to enhance SWP prediction accuracy in almond orchards.

This research aims to fill this gap by developing a comprehensive RF model incorporating diverse data types to enhance SWP prediction accuracy in almond orchards combining satellite imagery with soil, vegetation, and meteorological factors. This work seeks to advance the precision irrigation management in almond orchards by developing a robust machine learning model; integrating multiple data sources and leveraging advanced remote sensing technologies to provide a more accurate and scalable solution for predicting the plant water status.

2. Materials and methods

2.1. Study area description

The research was conducted in a commercial almond orchard near Corning, California, USA (39° 57′ 18.72″ N, 122° 14′ 49.2″ W). Fig. 1 provides an overview of the study area at Esteve Ranch near Corning, California, USA. The left side of the figure shows the orchard's location within California, marked by red pins. The right side of the figure is a detailed map of the orchard, indicating the locations of eight monitoring sites (C230–1 through C230–8) and the SWP tree monitoring locations marked with green dots. According to the Köppen climate classification, the region experiences a warm Mediterranean climate characterized by abundant sunshine and an annual average temperature of 16.6 °C, ideal for almond cultivation. The soil types in the area include sandy clay loam and clay loam. Additional site details have been documented by Peddinti and Kisekka (2022). The orchard comprises fields planted with three almond varieties: Nonpareil, Monterey, and Butte. These trees are 12 years old. These varieties were chosen for their commercial importance, with Nonpareil being highly valued for its superior shelling

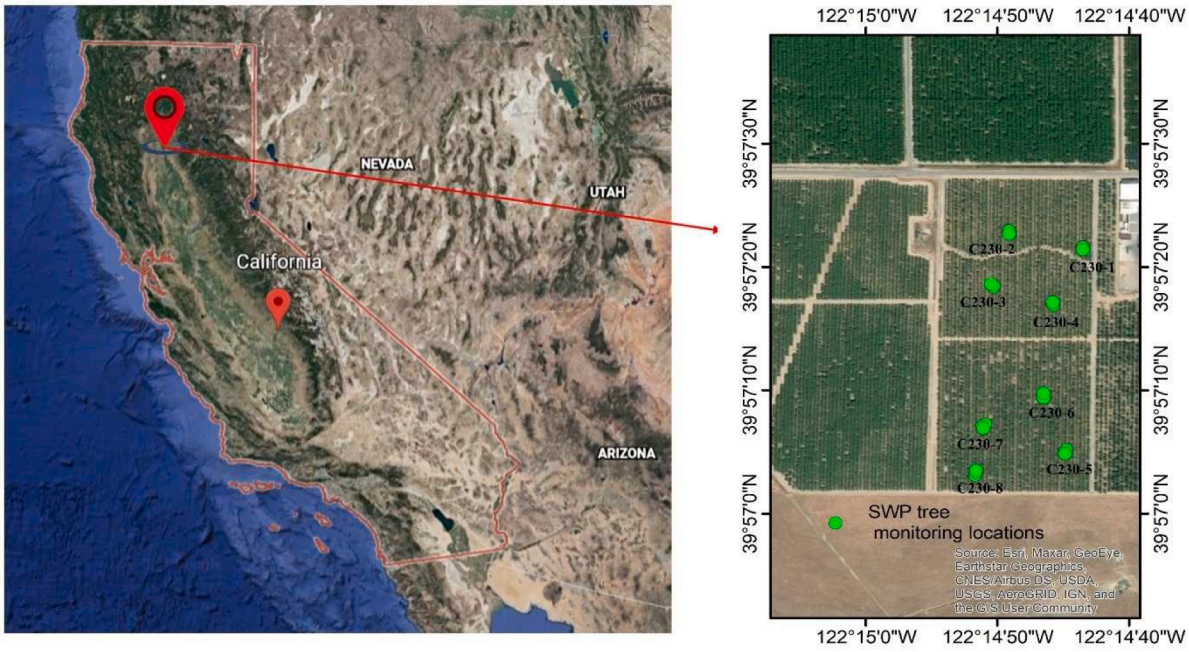


Fig. 1. The study area at Esteve Ranch near Corning, California, USA, shows the locations of eight monitoring sites and monitoring almond trees at each site, which are labeled C230–1, C230–2, C230–3, C230–4, C230–5, C230–6, C230–7, and C230–8.

characteristics and high market demand, and Monterey and Butte serving as critical pollinators and contributors to overall yield stability.

Irrigation was managed using a combination of micro-sprinkler and surface drip irrigation systems. During the growing season, irrigation schedules were based on real-time data from an eddy covariance system (Peddinti and Kisekka, 2022) deployed in the study area, which measured evapotranspiration (ET) at the field scale. This approach provided an accurate estimation of crop water demands, allowing precise adjustments to irrigation volumes. Specifically, a deficit irrigation strategy was implemented during the hull split period (mid-July to mid-August) to induce moderate water stress, which mitigates the risk of hull rot and optimizes water use efficiency. The total seasonal water application ranged from 783 mm to 944 mm, depending on the year's climatic conditions.

2.2. Stem water potential measurements

The SWP values of the monitored almond trees were measured using a pressure chamber technique, a widely accepted method for determining plant water potential. For SWP measurements, sun-exposed and fully expanded leaves were selected. To ensure consistency and minimize variability, a reflective plastic bag was used to cover the selected leaf from the lower canopy, which was shaded prior to measurement. The bagged leaf was left undisturbed for at least one hour to allow sufficient time for the water potential in the stem to equilibrate. Following this, the leaf, still enclosed within the plastic bag, was detached from the tree and immediately placed in the pressure chamber. The pressure was gradually applied until water exuded from the leaf petiole, and this pressure was recorded as the SWP value. A total of 24 almond trees were monitored across eight locations (Fig. 1), with three leaves per tree sampled during each measurement event. Measurements were taken at solar noon, between 12:30pm and 3:00pm, to standardize readings and minimize diurnal variability. To further reduce variability and potential human error, all SWP measurements were conducted by the same operator over the three-season experimental period. The SWP values were compared against established agronomic thresholds for almonds developed by (Fulton et al., 2014) where values between 0 to −0.6 MPa indicated no stress, −0.6 to −1.0 MPa represented low stress, −1.0 to −1.4 MPa corresponded to mild stress, and −1.4 to −1.8 MPa reflected moderate stress. Values more negative than −1.8 MPa were classified as severe stress, which could result in significant physiological limitations and potential yield reductions if prolonged. These thresholds provided a basis for interpreting water stress levels under varying irrigation and environmental conditions across the study period, facilitating a detailed analysis of the relationship between applied irrigation amounts and SWP dynamics (Fulton et al., 2014; Goldhamer and Ferees, 2001).

2.3. Climate and soil data

The meteorological data were collected from two different locations: a nearby (10 km) CIMIS station (ID: 222) and an eddy covariance (EC) flux tower situated within the study area (Peddinti and Kisekka, 2022). The data considered for the analysis averaged between 12pm and 3pm and included air temperature, relative humidity, wind speed, solar radiation, and vapor pressure deficit. Meteorological data for the 2019 season were collected from a nearby CIMIS station, located approximately 10 km from the flux tower. The flux tower was installed in 2020; therefore, data for the 2020 and 2021 seasons were directly obtained from the flux tower. Due to the proximity of the CIMIS station and the lack of significant differences in environmental conditions between the two locations, the 2019 data are considered representative of the site. Detailed descriptions of the flux tower and sensors can be found in (Peddinti and Kisekka, 2022). Soil bulk density was estimated using data from the Gridded Soil Survey Geographic Database (gSSURGO). The database provides bulk density values for various soil layers, which were averaged across the top 30 cm to generate the soil bulk density map. These values were processed at a 30-meter spatial resolution, and the bulk density at specific almond tree locations was extracted based on their geographic coordinates. This map was then used for analysis in the study. Evaporation fraction (EF) was estimated using the pySEBAL model for the three seasons from 2019 to 2021 with Landsat data, and values were extracted at all monitored almond tree locations (Peddinti and Kisekka, 2022). Normalized Difference Vegetation Index (NDVI) values were estimated using Landsat imagery, as calculated with Eq. (1).

$$NDVI = \frac{NIR - Red}{NIR + Red} \quad (1)$$

where *NIR* is the reflectance in the near-infrared band, and *Red* is the reflectance in the red band.

The methods for estimating EF and NDVI are discussed in detail in (Peddinti and Kisekka, 2022). Soil water content (SWC) values at an average depth of 45 cm were obtained from neutron probe measurements at eight monitoring sites within the study area (Fig. 1). These measurements were collected during the same period as the SWP data to ensure consistency and enable accurate correlation between soil and plant water status.

2.4. High resolution aerial imagery

To test the Random Forest (RF) model for predicting spatial maps within the study region, we utilized high-resolution aerial imagery with a 0.5 m resolution to predict the spatial maps of SWP. Ceres Imaging, Inc. provided aerial imagery acquisition and preprocessing (https://www.ceresimaging.net/). The airborne campaign included 11 flights, with flight heights ranging from 1918 m to 1951 m. During the campaign, both thermal and multispectral images were captured at varying resolutions. Images were captured between 11:00AM and 4:00PM (PST) using a FLIR A65 thermal sensor (FLIR Systems, Wilsonville, OR, USA) and a constellation of VNIR IDS camera systems (https://www.ids-imaging.us/contact.html). The thermal sensor used a 13-mm lens with a field of view (FOV) of 45° x 37°, capturing images with a resolution of 1575 (nrow) x 562 (ncol) pixels. The spectral response range for these images was between 7.5 to 13 Âµm in wavelength. The spatial resolution of the images acquired was nearly identical, with thermal and multispectral images ranging from 0.6 to 0.7 m. To maintain consistency and accuracy, the images were resampled to ensure a 0.5 m resolution. The detailed processing of the imagery, including calibration, alignment, and any preprocessing steps, can be found in the paper by (Peddinti and Kisekka, 2022).

2.5. Soil pixel removal in aerial imagery

The most significant interfering objects in the aerial images were soil pixels, which needed to be removed to obtain a complete representation of the almond canopy. To achieve this, the NDVI was utilized for each date, and the histogram of pixel values was created. The Otsu method (Otsu, 1979) was then applied to determine the optimal threshold values for separating soil from canopy pixels. This method calculates the threshold that minimizes interclass variance and maximizes intraclass variance, effectively distinguishing soil pixels from vegetation (Kim et al., 2018). In this study, NDVI values below 0.75 were classified as soil, while values above 0.75 were classified as almond canopy.

2.6. Random forest classifier training, validation, and overfitting

Conventional machine learning algorithms often overlook the spatial-temporal correlations within data, leading to inaccurate spatio-temporal predictions. This issue is exacerbated by overfitting during model construction and the objective error evaluation process, making spatial predictions particularly problematic. To address these limitations, the CAST package (Meyer et al., 2018) was developed to build RF models that account for spatiotemporal interdependence in prediction tasks. This study implemented the RF model using the R package CAST (https://cran.r-project.org/web/packages/CAST/index.html) to predict SWP at various spatial and temporal scales. An RF is a non-parametric ensemble learning method composed of multiple weak decision trees suitable for classification and regression tasks. The model construction involved selecting random samples with replacements from measured SWP values of 24 almond trees at eight monitoring sites over three seasons (2019 to 2021). These samples were used for training and validation. The data were split into in-bag samples for training the trees and out-of-bag samples for internal cross-validation to estimate the learning process error, referred to as the out-of-bag error. Each tree in the forest was constructed independently with two key hyperparameters: the number of trees (Ntree) set to 500, and the number of features used to split each node (Mtry) set to 10.

Meteorological variables, soil properties, and EF and NDVI derived from Landsat imagery were used as covariates in the RF regression model. When SWP measurements were taken at each location (C230–1 to C230–8), meteorological variables such as average solar radiation, wind speed, air temperature, relative humidity, and vapor pressure deficit were considered between 12pm and 3pm (PST). Additionally, soil parameters like the spatial distribution of bulk density (BD) and SWC at a 0.45 m depth (from neutron probe measurements taken over three seasons) were used as predictor variables. During the model training phase, daily linear interpolated ET, NDVI, BD, and SWC values were derived over a three-year period and used as predictor variables for the corresponding SWP measurement dates. For model validation, k-fold cross-validation (CV) was employed, a popular strategy allowing to estimate model performance using data not utilized during training (Kisekka et al., 2022; Meyer et al., 2018; Phinzi et al., 2021; Shanley et al., 2021). Random 10-fold CVs were conducted to evaluate the model's performance on random subsets of the total dataset. The SWP data were divided into 10 folds of equal size using stratified random sampling, ensuring that the distribution of the response variable in each fold matched that of the entire dataset. Models were trained on all but one-fold of data, with the held-back fold used to test model performance, thus assessing model fit in both spatial and temporal dimensions. The 10-fold CV results were compared to target-specific validation results. A forward feature selection (FFS) algorithm was used alongside target-oriented validation to remove ineffective predictors, enhancing model performance. Detailed procedures for cross-validation and addressing overfitting are available in (Meyer et al., 2018).

2.7. Statistical evaluation

The accuracy of SWP values predicted by the RF model was evaluated against measured SWP values using the FITEVAL (Ritter and Muñoz-Carpena, 2013) (https://abe.ufl.edu/faculty/carpena/software/FITEVAL.shtml) software. Statistical indicators such as root mean squared error (RMSE), Kling-Gupta efficiency (KGE), and the Nash-Sutcliffe efficiency coefficient (NSE) were used for the goodness-of-fit analysis. RMSE quantified the average error, while KGE assessed bias, correlation, and variability, with higher values indicating better performance. NSE values were categorized into four levels: very good, good, acceptable, and unsatisfactory, to evaluate model reliability. FITEVAL also used block bootstrapping (Politis and Romano, 1994) to estimate the NSE probability distribution, identify biases, and test the null hypothesis of unacceptable model fit (NSE $<$ threshold). This comprehensive evaluation highlighted the RF model's predictive performance and areas for improvement.

3. Results

3.1. Stem water potential (SWP) dynamics

Fig. 2 presents the seasonal variation in stem water potential (SWP) measurements for almond trees at eight monitoring locations from April to October over three consecutive years (2019–2021). The SWP values relative to the baseline (Fig. 2a) indicate deviations from optimal conditions, while direct SWP measurements (Fig. 2b) provide an absolute quantification of tree water status alongside recorded irrigation applications. During the early growing season (April–May), SWP deviations were minimal, ranging from 0 to −0.6 MPa, while direct SWP measurements remained within −0.5 to −1.0 MPa, indicating an absence of significant water stress. Irrigation applications during this period were

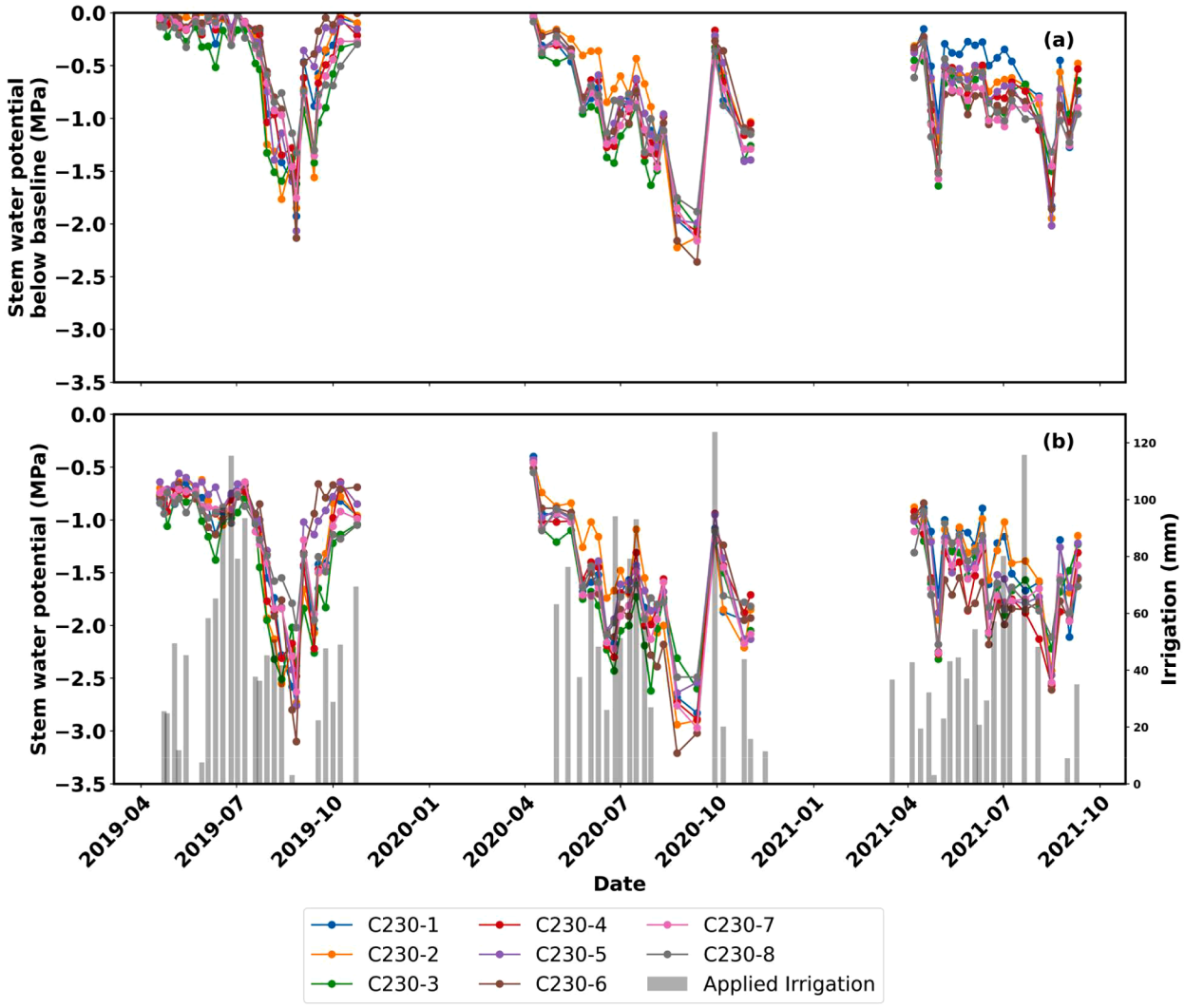


Fig. 2. Weekly stem water potential (SWP) measurements and applied irrigation for Almond trees at eight monitoring locations (C230–1 to C230–8) from April to October (2019–2021). (a) SWP values relative to the baseline indicate deviations from optimal conditions, and (b) direct SWP measurements with corresponding applied irrigation data.

relatively low, typically below 40 mm per week. As the season progressed into June and July, SWP deviations reached −1.0 to −2.0 MPa, while direct SWP values ranged from −1.5 to −2.5 MPa across all locations. During this period, irrigation inputs increased, often exceeding 100 mm per week, yet SWP values continued to decline. In the mid-season (July–August), corresponding to the hull split phase, SWP values frequently entered the mild stress range (−1.0 to −1.4 MPa), with occasional measurements approaching the moderate stress threshold (−1.4 to −1.8 MPa), despite sustained irrigation applications. During the late season (August–September), as crop water demand decreased, SWP values exhibited partial recovery, fluctuating between −1.0 and −1.5 MPa, with a corresponding reduction in irrigation volumes. However, some locations recorded SWP values below −2.5 MPa, indicating periods of more pronounced water stress.

3.2. Meteorological conditions

Fig. 3 illustrates various meteorological parameters averaged between 12 and 3PM from 2019 to 2021, aligning with the period when SWP measurements were taken in almond trees. Each subplot represents different climatic variables: (a) solar radiation, (b) vapor pressure deficit (VPD), (c) air temperature, (d) relative humidity, and (e) wind speed. Solar radiation (Fig. 3a) exhibits a clear seasonal pattern, with peak values reaching approximately 1000 W/m^2 in summer (June–August) and declining to below 200 W m^{-2} during winter (December–February). VPD (Fig. 3b) follows a similar trend, peaking at around 2.5 kPa in summer and dropping below 0.5 kPa in winter. Air temperature (Fig. 3c) increases from early spring, reaching maximum values of around 35 °C in summer, before decreasing towards winter with minimum values below 5 °C. Relative humidity (Fig. 3d) varies inversely with temperature and VPD, fluctuating between 20 and 40 % in summer and increasing above 80 % in winter. Wind speed (Fig. 3e) shows a more variable trend, with sporadic peaks reaching 3 to 5 m s^{-1} during the summer months, while remaining below 1.5 m s^{-1} for most of the winter period.

3.3. Linear regression analysis between SWP with NDVI, SWC, and EF

The linear regression analysis presented in Figs. 4–6 quantifies the relationships between SWP and three key variables: Normalized Difference Vegetation Index (NDVI), soil water content (SWC), and evaporation fraction (EF). Fig. 4 illustrates a positive correlation between SWP and NDVI across all monitoring locations, indicating that higher NDVI values, representing healthier vegetation, are associated with higher (less negative) SWP values, reflecting lower water stress. The coefficient of determination (R^2) values range from 0.26 to 0.38, while

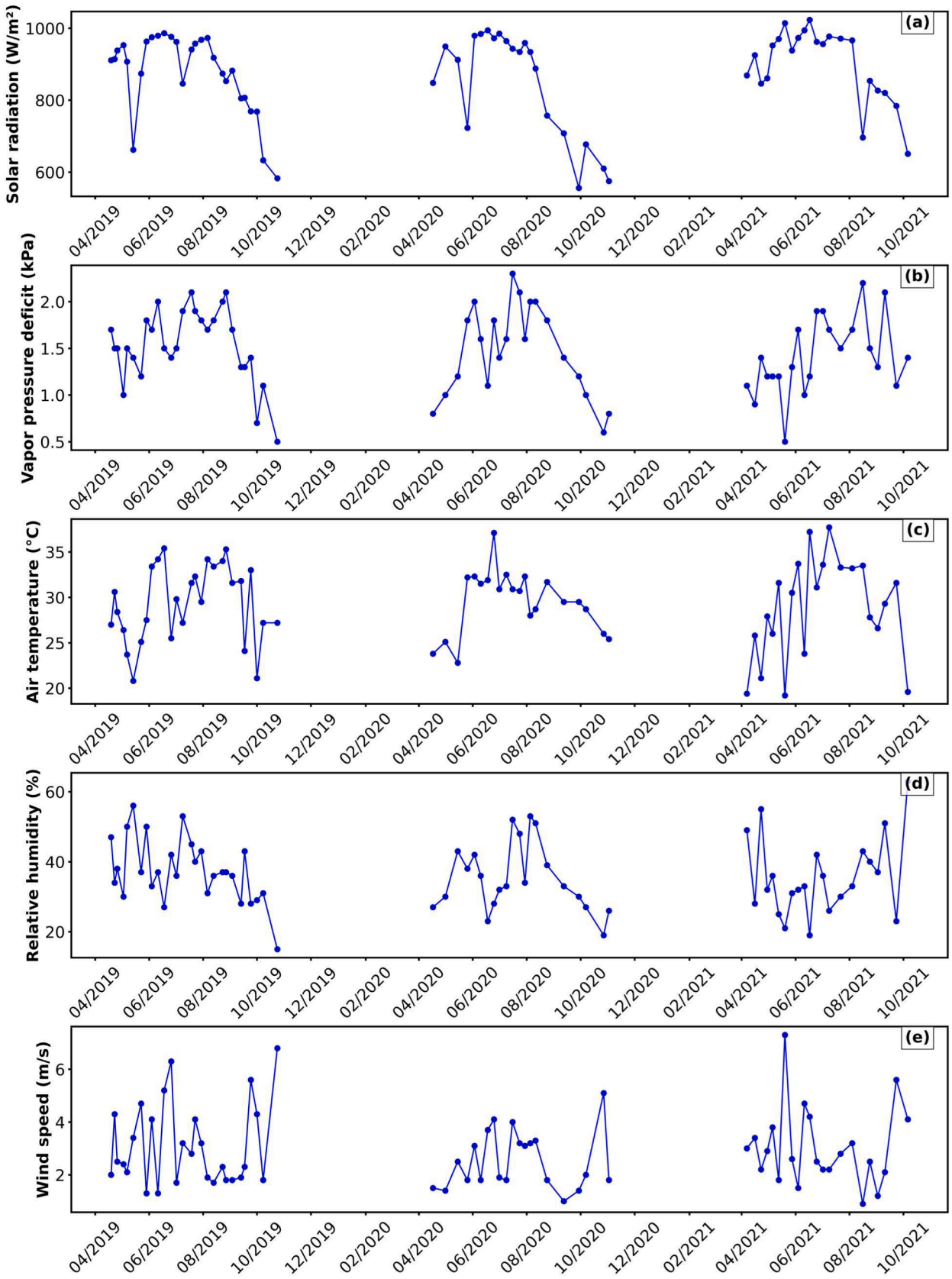


Fig. 3. The average values of various meteorological parameters recorded between 12 and 3PM during the growing seasons (April to October) of 2019, 2020, and 2021. It includes (a) solar radiation (W/m^2), (b) vapor pressure deficit (kPa), (c) air temperature (°C), (d) relative humidity (%), and (e) wind speed (m/s).

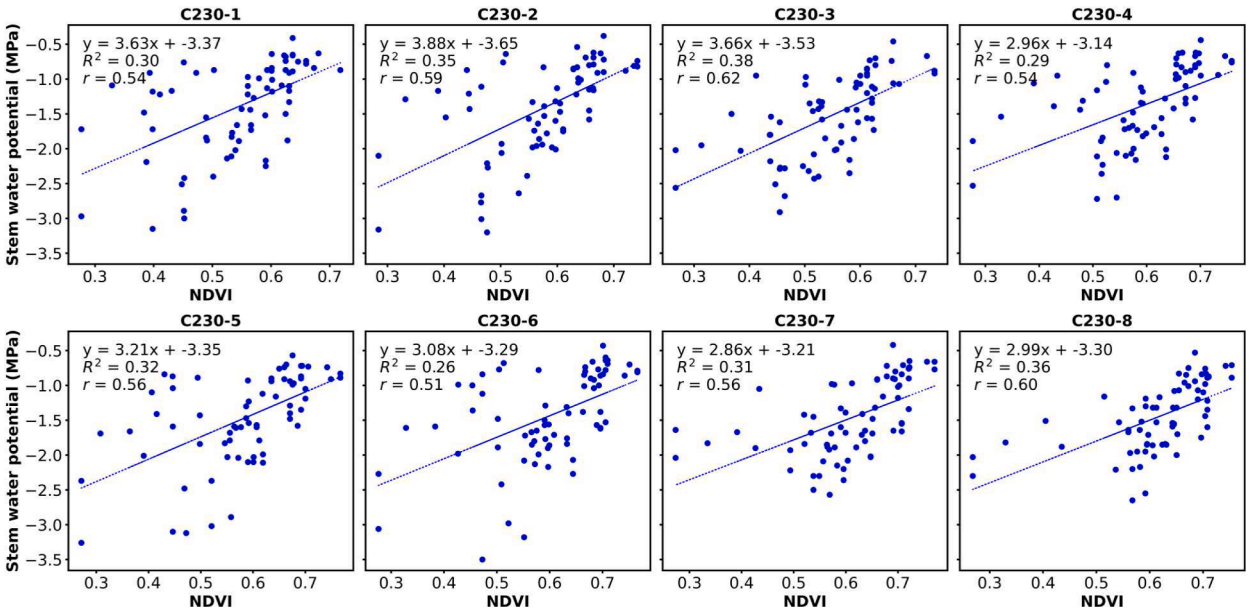


Fig. 4. Linear correlations between the normalized difference vegetation index (NDVI) extracted from Landsat imagery at monitoring almond trees, and measured SWP values at C230–1 to C230–8 monitoring sites. Here, R^2 represents the coefficient of determination, and 'r' denotes Pearson's correlation coefficient.

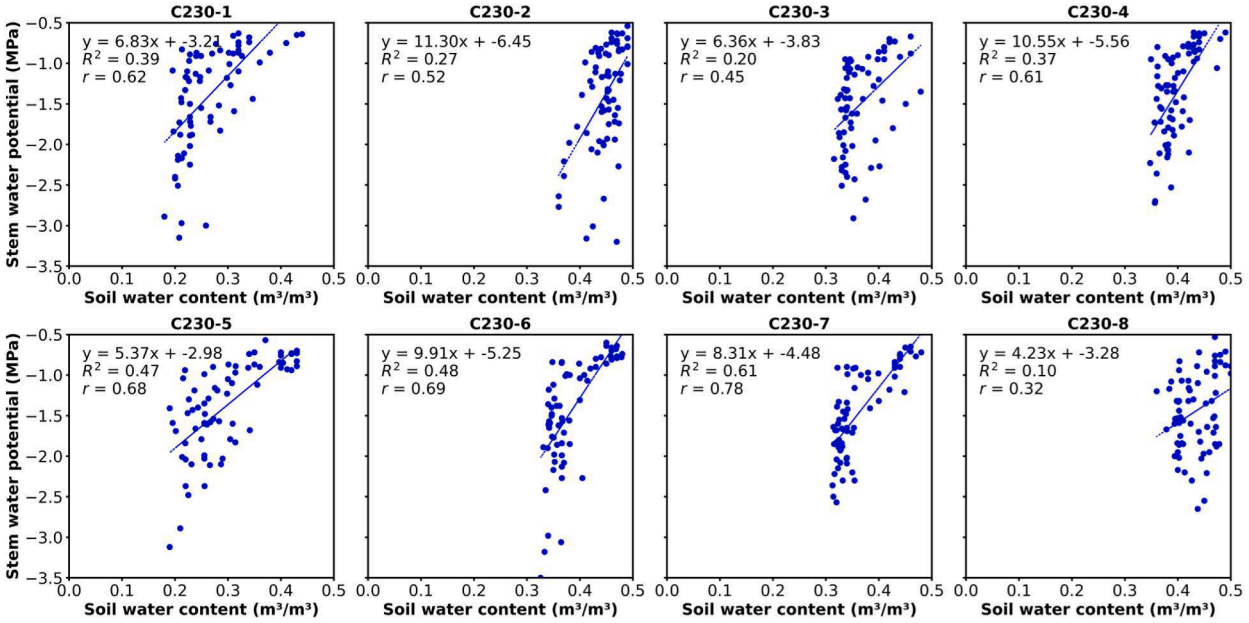


Fig. 5. Linear correlations between the soil water content from neutron probes at 45 cm depth, and measured SWP values at C230–1 to C230–8 monitoring sites.

Pearson's correlation coefficient (r) values range from 0.51 to 0.62, suggesting a moderate relationship between NDVI and SWP. Despite the positive correlation, the relatively low R^2 values indicate that NDVI alone does not fully account for the observed variability in SWP across locations. Fig. 5 illustrates the relationship between SWP and SWC, demonstrating a positive correlation at all locations. The R^2 values range from 0.10 to 0.61, and Pearson's r values range from 0.32 to 0.78, indicating a stronger association compared to NDVI. Higher soil water content generally corresponds to higher (less negative) SWP values, suggesting lower water stress. However, the variation in R^2 values across different locations suggests that site-specific factors, such as soil properties and root distribution, influence this relationship. Fig. 6 examines the relationship between SWP and EF, revealing a weaker correlation compared to NDVI and SWC. The R^2 values range from 0.01 to 0.23, while Pearson's r values range from 0.10 to 0.48. Although the regression slopes indicate that higher EF values, representing increased actual evaporation rates, are associated with improved water status, the weak correlations suggest that EF alone is not a strong predictor of SWP.

3.4. Performance evaluation of RF model in predicting SWP

Fig. 7 presents an in-depth evaluation of the RF model's performance in predicting SWP in almond orchards. This comprehensive analysis compares the RF model predictions with SWP measurements obtained using a pressure chamber (PC) through various statistical assessments. The strong correlation observed with a Nash-Sutcliffe Efficiency (NSE) of 0.91 [0.87 - 0.94], indicates an excellent fit between the predicted and observed values (Fig. 7a). The Root Mean Square Error (RMSE) of 0.17

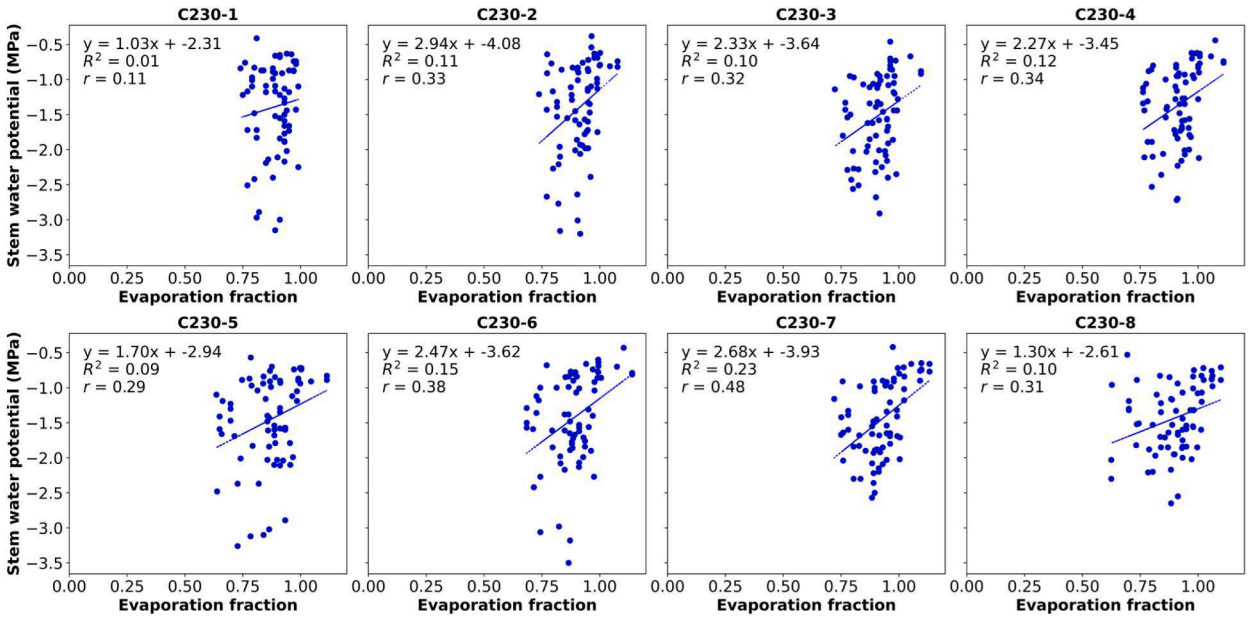


Fig. 6. Linear correlations between the evaporation fraction (EF) estimated using pySEBAL model using Landsat imagery and extracted at monitoring almond trees, and measured SWP values at C230–1 to C230–8 monitoring sites.

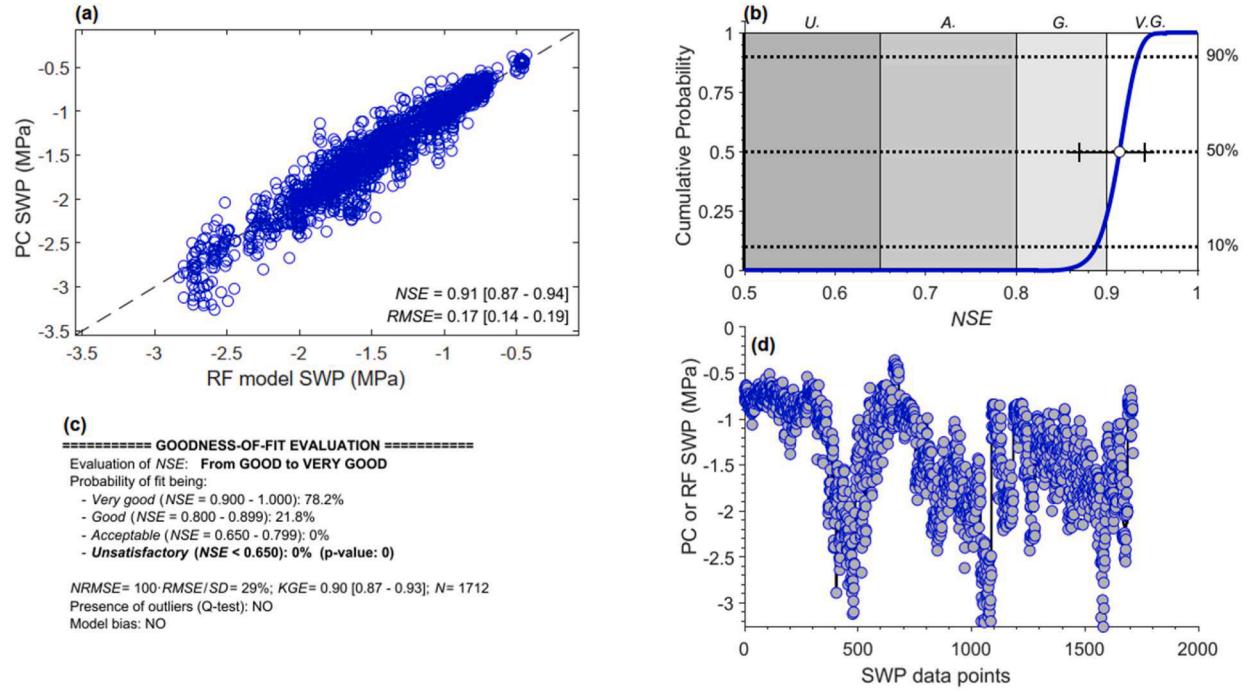


Fig. 7. Assessment of goodness-of-fit and regression outcomes between mid-day stem water potential measured by PC devices and predicted by RF model for the period of three seasons from 2019 to 2020. The detailed graphical representations depicting (a) the regression analysis between RF model and PC measured SWP data, (b) the cumulative probability of NSE, with the median value indicating the reported NSE, (c) a FITEVAL model report encompassing hypothesis testing outcomes, identification of outliers, and sensitivity analysis concerning model bias, and (d) a time series plot illustrating the correlation between SWP values from RF model and PC measurements.

[0.14 - 0.19] MPa further demonstrates the model's precision. The alignment of the regression line with the 1:1 line signifies that the RF model predictions are in close agreement with the actual measurements, confirming the model's robustness in predicting SWP. The NSE cumulative probability plot (Fig. 7b) reveals that 78.2 % of the model predictions fall within the "very good" category (NSE $\geq$ 0.90), and 21.8 % are classified as "good" (0.80 $\leq$ NSE $<$ 0.90). Notably, there are no predictions in the "acceptable" or "unsatisfactory" categories (NSE $<$ 0.65), underscoring the model's consistent performance across different data points. The RMSE of 0.17 MPa (Fig. 7c) quantifies the average deviation of predictions from actual measurements, while the normalized RMSE (NRMSE) of 29 % and the Kling-Gupta Efficiency (KGE) of 0.90 [0.87 - 0.93] further attest to the model's accuracy. The absence of model bias is confirmed by the Q-test, which detects no significant outliers, ensuring the reliability of the RF model. The temporal correlation (Fig. 7d) displays a high degree of temporal agreement, indicating

that the RF model effectively captures the dynamic changes in SWP over time. Overall, the RF model demonstrates exceptional accuracy and reliability in predicting SWP, as evidenced by the strong linear correlation, high NSE, low RMSE, and robust performance metrics.

3.5. Variable importance of random forest model

The analysis of variable importance in the RF model's prediction of SWP in almond trees is illustrated in Fig. 8. This figure shows the importance of various variables across the training, validation, and overfitting stages. During the training stage, air temperature (AT) emerged as the most significant variable with an importance of 100 %, followed by NDVI (80 %), wind speed (WS) (60 %), solar radiation (SolRad) (50 %), and soil water content (SWC) (40 %). In the validation stage, the variable importance rankings remained largely consistent, with AT (100 %), NDVI (80 %), and WS (60 %) continuing to show high importance. During the overfitting stage, a notable shift in variable importance was observed. Variables such as evapotranspiration fraction (EF) (80 %) and SWC (40 %) gained prominence, while NDVI's importance decreased to the point of being completely removed. Fig. 9 presents R^2 values across multiple model runs, demonstrating the effect of including different numbers of variables. Models with fewer variables showed higher variability in R^2 values, whereas models including around 8–9 variables exhibited the highest and most stable R^2 values. This indicates that incorporating a sufficient number of relevant variables improves model stability and predictive accuracy.

3.6. Spatial variability of stem water potential

The spatial maps, created for 11 dates, provide a detailed view of SWP variation (Fig. 10) before and after the almond hull split period. The dates covered in the spatial maps are 6/22/2020, 7/6/2020, 7/10/2020, 7/11/2020, 7/12/2020, 7/13/2020, and 7/14/2020, which are before the hull split period. The subsequent dates, 7/22/2020, 7/23/2020, 7/24/2020, and 7/25/2020, fall after the hull split period. The spatial maps indicate significant variations in SWP across different parts of the orchard. Before the hull split, SWP values are more varied, with noticeable stress patches indicated by more negative SWP values (closer to −2.0 MPa). This variation can be attributed to different microclimatic conditions, soil moisture availability, and the physiological status of the

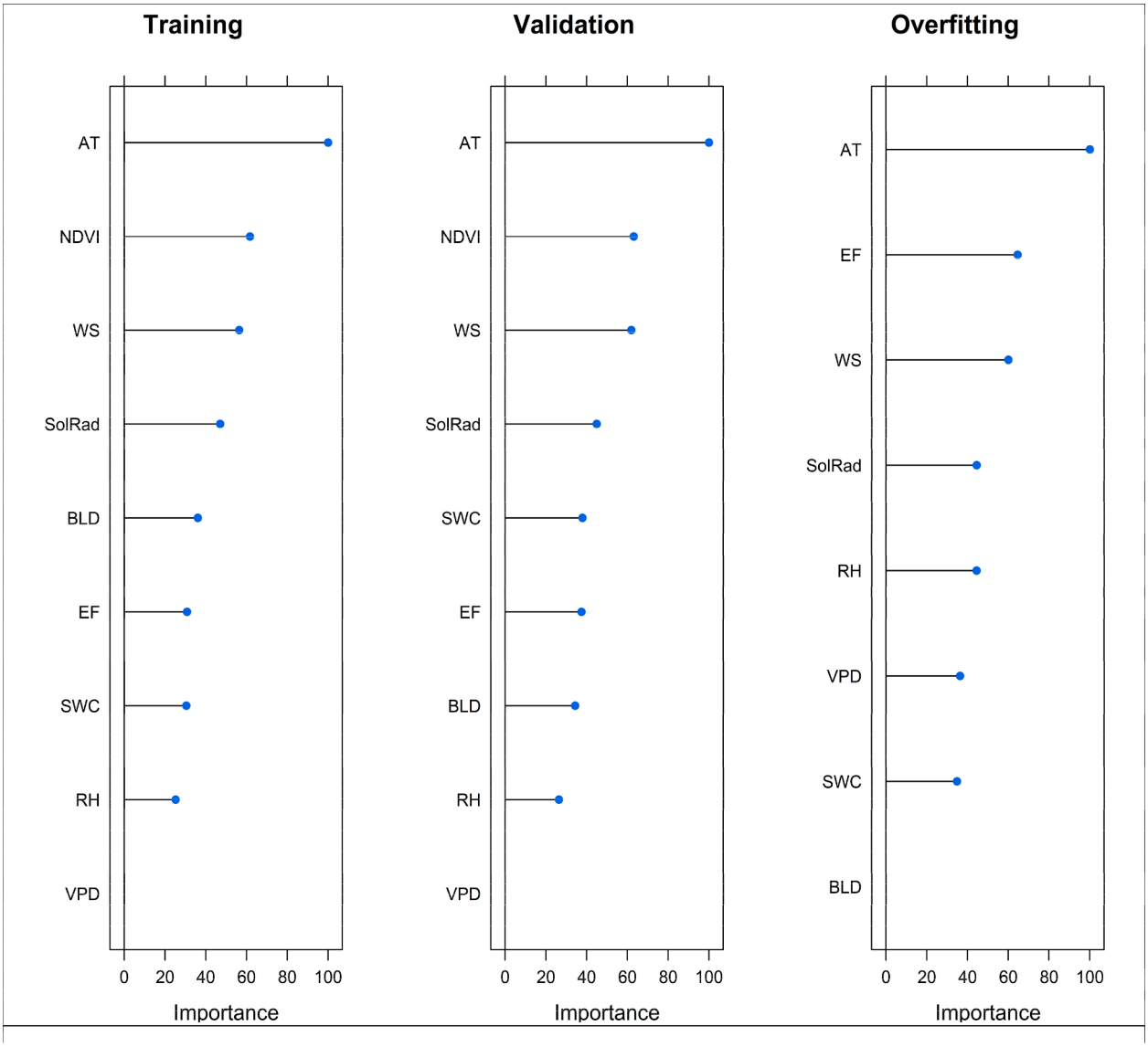


Fig. 8. Variable importance parameters for the RF model at training, target-oriented validation, and overfitting. Here the parameters indicated as follows: NDVI is normalized difference vegetation index, SWC is soil water content, AT is air temperature, EF is evaporation fraction, SolRad is solar radiation, BLD is soil bulk density, WS is wind speed, RH is relative humidity, and VPD is vapor pressure deficit.

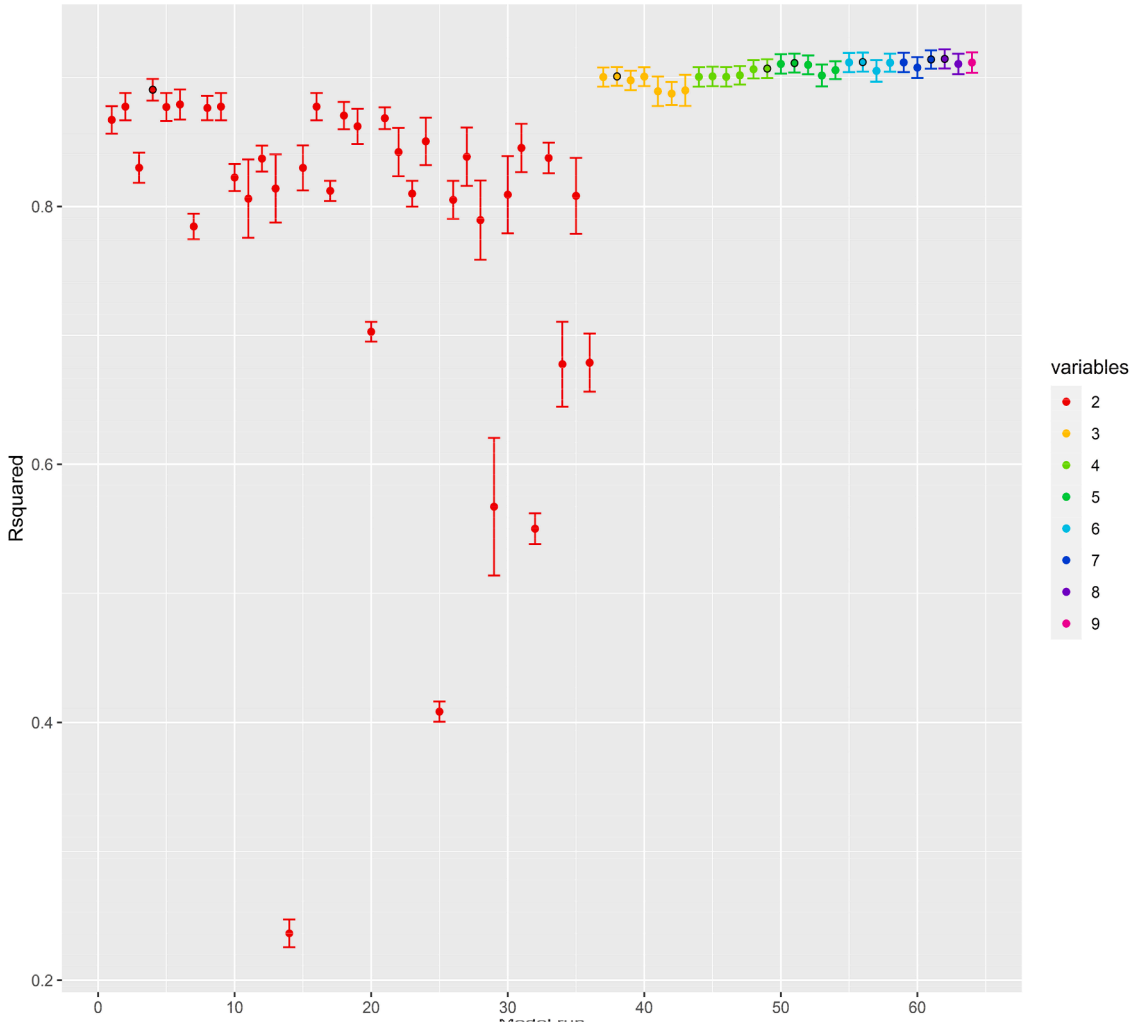


Fig. 9. Overfitting RF model performance with important variables indicated with black circles based on the highest R^2 model.

trees. As the hull split approaches, it is critical to manage water stress to ensure the health of the trees and the quality of the nuts. After the hull split, the maps from 7/22/2020 to 7/25/2020 show a reduction in severe water stress areas, indicating effective water management practices. This period requires careful irrigation management to maintain moderate stress levels, which helps in reducing the incidence of hull rot and ensuring the nuts mature properly. Overall, the spatial prediction maps created using the RF model demonstrate the temporal and spatial dynamics of SWP in almond orchards, highlighting the importance of precise water management before and after the hull split period. These maps serve as valuable tools for growers to monitor tree water status and make informed irrigation decisions, ultimately improving crop health and yield.

4. Discussion

Effective water management is critical for maintaining tree health, optimizing yield, and ensuring efficient harvest operations in almond orchards (Smith et al., 2022). One widely adopted approach is regulated deficit irrigation (RDI), which strategically applies mild water stress to enhance nut maturity and reduce hull rot incidence (Cirhigiri, 2022; Smith, 2021). The SWP trends observed in Fig. 2 reflect the modulation of tree water status in response to phenological stages and irrigation practices. Early-season (April–May) low stress ensured optimal vegetative and reproductive development, with SWP values remaining within acceptable ranges. As the season progressed, SWP declined during June and July, aligning with peak evaporative demand despite increased irrigation inputs. This condition is agronomically acceptable, as mild water stress does not significantly impact yield and may improve water use efficiency (Moriana et al., 2012; Olivo et al., 2009).

During the mid-season (July–August), which corresponds to the hull split phase, SWP values indicated mild to moderate water stress, likely a result of targeted irrigation management aimed at reducing hull rot risks. This aligns with previous findings that controlled stress during hull split can optimize water use without compromising nut quality (Stewart et al., 2011). However, occasional excursions into higher stress conditions (SWP below −1.8 MPa) were observed. Prolonged exposure to such stress should be avoided, as it can result in yield penalties, canopy degradation, and increased risks of partial defoliation or limb dieback. In the late season (August–September), SWP showed partial recovery, indicating effective irrigation adjustments to balance crop demand and water supply. However, the presence of occasional mild stress highlights the need for careful irrigation scheduling to prevent unnecessary yield losses. The three-year dataset highlights an effectively managed irrigation strategy, characterized by adequate water availability in the early season, controlled stress during the mid-season, and partial recovery in the late season, all of which contributed to optimizing tree performance while enhancing water use efficiency.

The random forest (RF) model's variable importance analysis provides valuable insights into the key factors influencing SWP in almond trees. Among all variables, air temperature (AT) emerged as the most significant driver of water stress, highlighting its strong influence on

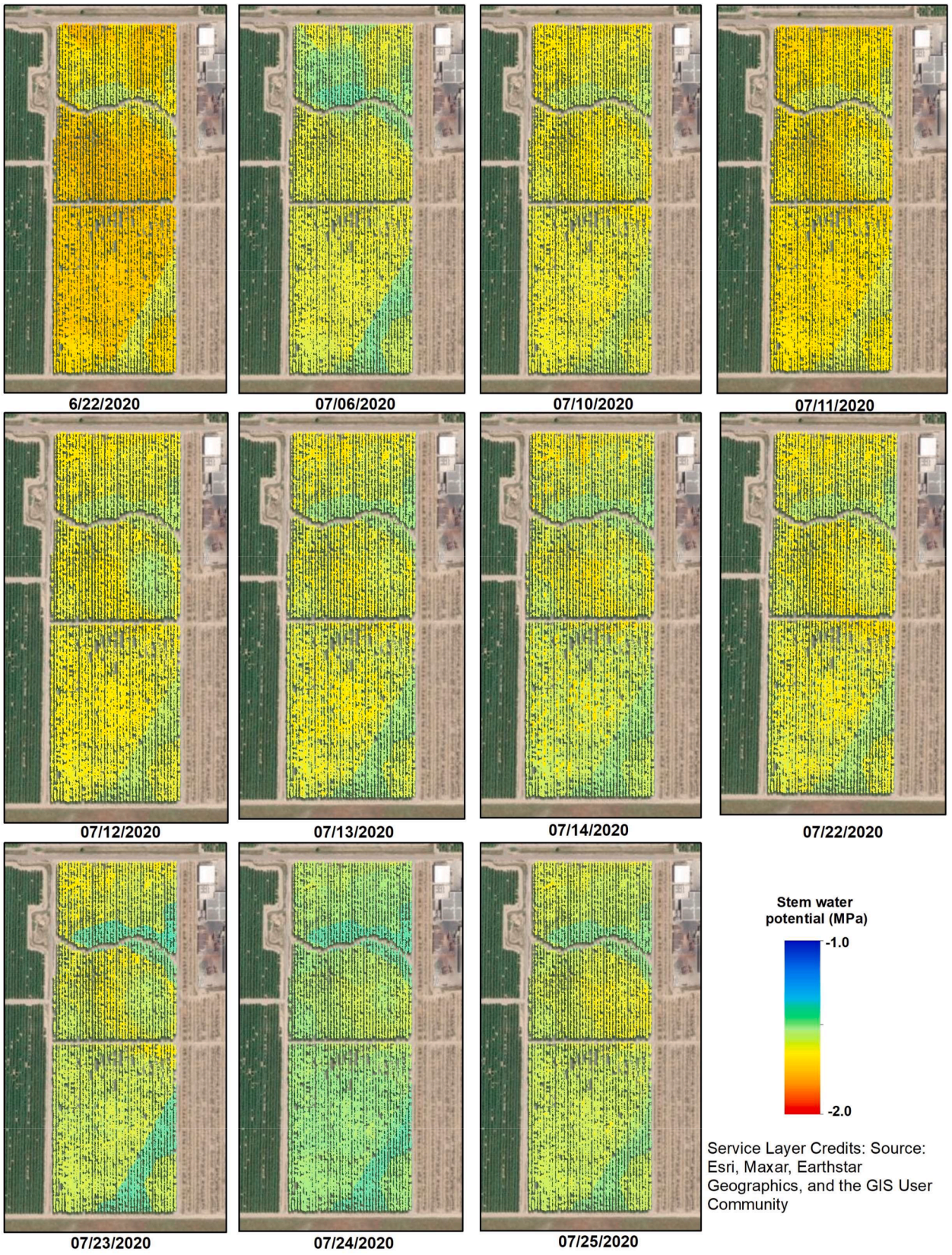


Fig. 10. Spatial variability of the midday stem water potential values at different dates predicted using overfitting RF model.

plant physiological responses. The considerable contribution of NDVI underscores the importance of vegetation health in assessing tree water status, as healthier canopies typically manage water stress more effectively (Sarvakar and Thakkar, 2024). Additionally, wind speed (WS), solar radiation (SolRad), and soil water content (SWC) played meaningful roles, reflecting the complex interactions between climatic and soil factors in influencing SWP.

The consistency of variable importance across the training and validation stages suggests that the RF model has robust predictive capabilities and is not overly sensitive to dataset variations (Huang and Boutros, 2016). However, during the overfitting stage, a shift in variable importance was observed, with evapotranspiration fraction (EF) and SWC gaining prominence while NDVI was completely removed. This shift likely reflects the model's tendency to overemphasize less relevant or more variable features when it becomes too complex. The exclusion of NDVI in this stage suggests that its relationship with SWP remains stable and less prone to random fluctuations, making it less susceptible to overfitting effects. The patterns observed in Fig. 9 indicate that an optimal number of 8–9 variables results in the most accurate and stable predictions. Models with fewer variables exhibited greater variability in R^2 values, suggesting reduced stability, whereas those incorporating too many variables introduced noise and potential overfitting. The diminishing returns in model accuracy with increasing variables emphasize the need for a carefully optimized feature selection strategy to maximize predictive accuracy while minimizing the risk of overfitting.

The RF model's ability to capture non-linear interactions and complex dependencies among multiple variables highlights differences between linear regression results and variable importance in the RF model. Although linear regression shows a weaker correlation for EF, the RF model assigns high importance to both NDVI and EF (80 %) in predicting SWP, while SWC has lower importance (40 %). This suggests that NDVI and EF play significant roles in predicting SWP when combined with other factors, likely due to their complex interactions with environmental variables that influence tree water status. The linear regression analysis between SWP and NDVI explained approximately 38 % of the variance. However, in the RF model, NDVI was identified as the most important variable in both the training and validation phases. For spatial prediction, NDVI was excluded from the model, possibly because EF was a more relevant predictor with a significance of 80 %. Since NDVI is a variable used in EF calculations, the RF model may have prioritized EF over NDVI in spatial predictions.

These findings are consistent with previous studies. (Lin et al., 2020) reported that NDVI had less than 10 % importance in RF models for spatial predictions in cotton crops. Similarly, (Zhao et al., 2017a, 2015) investigated the linear relationship between SWP and NDVI in almond orchards over a three-week period and found no clear correlation between canopy NDVI and SWP. (Poblete et al., 2017) observed a linear correlation ($R^2 = 0.35$) between SWP and NDVI in vineyards in Chile, aligning with the findings of the current study. While the relationship between SWP and NDVI, a measure of plant functional diversity, is well recognized in plant physiology, the underlying mechanisms governing ecosystem health are still not fully understood. In almond orchards, particularly during the leaf development stage, low NDVI values are often associated with high SWP, suggesting that plant water potential dynamics are influenced by phenological stages. The analysis also provides critical insights into the factors that most significantly influence SWP predictions. The high importance of AT, NDVI, and WS during training and validation highlights their fundamental role in determining tree water status. These variables likely capture key aspects of the microclimate and plant physiological responses that drive SWP variations. AT directly affects transpiration rates and overall plant water use, NDVI reflects plant health and vigor, and WS influences moisture loss from leaves, further contributing to fluctuations in SWP.

Comparative studies have shown the effectiveness of remote sensing and machine learning techniques in predicting SWP across various crops. For example, a study in olive orchards using high-resolution satellite images and machine learning reported an R^2 of 0.78 for RF models, indicating a strong prediction capability for olive water status (Garofalo et al., 2024). Another study focused on almond orchards, where RF models created high-resolution spatial maps of SWP, achieving an average R^2 of 0.47 and an RMSE of 0.27 MPa (Savchik et al., 2024). Compared to this study, our model not only has a lower RMSE but also suggests better overall prediction accuracy. The availability of soil water is a critical factor influencing the growth of almond plants. It is primarily controlled by the balance between water influx (infiltration and rainfall) and water outflow (evapotranspiration), which is, in turn, largely determined by the amount of water stored in the root zone. In the current study, the SWC is well correlated with SWP values, but the SWC parameter was omitted by the overfitting RF model. The reason for this could be that, once again, the EF is only indirectly related to the SWC in the soil. In accordance with the results of the linear regression in this study, (Abrisqueta et al., 2015) performed the multiple linear regression with SWC and VPD and found that for peach 72 % variance in SWP was present. (Intrigliolo et al., 2012) found significant linear relationships between maximum SWC and SWP in grapevines over three seasons at different irrigation treatments. Among the treatments, the early deficit treatment had an R^2 of 0.21, the rainfed treatment had an R^2 of 0.71, and the maximum irrigation treatment had an R^2 of 0.71. In non-irrigated vines, (Beslic et al., 2015) observed a linear relationship with an R^2 of 0.52 in bare soil and 0.45 in cover crops. These results show that at the deficit stage, the relationships between the SWP of crops and the available water are poor, compared to the high water available for the crops.

The overfitting RF model reveals that AT, and EF are the most important attributes for the spatial prediction of SWP in the study region. However, the independent linear correlation between EF and SWP is extremely low. In contrast, (Bellvert et al., 2021) demonstrated a statistically significant power relationship between actual evapotranspiration and SWP, with an R^2 of 0.68 in different varieties of almond rootstocks, and concluded that trees grafted on the least vigorous rootstocks had the lowest SWP values. These results suggest that rootstock selection also impacts SWP values in almond orchards. The relationship between SWP and temperature is crucial and complex. Plants employ various mechanisms to maintain SWP at a level that allows cells to function efficiently. Increased water concentration in cells causes them to expand, increasing their volume and ability to take up water and nutrients from the environment. Extreme soil and air temperatures at noon can alter the rate of water transport from the soil into the root and plant system, thereby reducing plant transpiration rates. In areas where plant transpiration cannot keep up with high EF demand, the RF model's strong influence on these parameters is evident at the spatial scale required to predict SWP (Irmak and Mutiibwa, 2010; S. Irmak and D. Mutiibwa, 2009). This influence highlights the importance of incorporating these factors into predictive models to ensure accurate and reliable SWP predictions across different environmental conditions.

The CAST package's forward feature selection (Meyer et al., 2018) capability in the RF model excludes counterproductive or insignificant variables, providing valuable information about variable importance in training, validation, and overfitting models. Based on R^2 evaluation criteria, the overfitting model used only 8 out of 9 variables. The R^2 values for spatial prediction range from 0.2 with two variables to greater than 0.9 with eight variables. This suggests that while the RF model performed better than linear models due to its ability to handle nonlinearity, careful selection of variables is essential to avoid overfitting. Overall, the study demonstrates the efficacy of using RF models to predict spatial and temporal SWP in almond orchards, emphasizing the significant roles of NDVI and EF, among other environmental variables. The model's ability to capture non-linear interactions and handle complex dependencies showcases its superiority over traditional linear regression methods. However, the tendency of the model to overfit highlights the need for careful variable selection and model tuning to ensure robust predictions. Future research should focus on refining these

predictive models by incorporating more diverse datasets across regions and crop types. Additionally, exploring the integration of real-time remote sensing data and advanced machine learning techniques could further enhance the accuracy and applicability of SWP predictions. Understanding the mechanistic relationships between SWP and key variables such as NDVI and EF at finer spatial and temporal resolutions will be crucial in advancing precision agriculture practices, ultimately leading to more efficient water management and improved crop yields.

Given the climatic and environmental similarities between California and other Mediterranean regions, such as southern Spain, where almond cultivation is significant, the findings of this study could have broader applicability (Arroyo et al., 2022; Vuppalapati, 2023; Yada et al., 2013). Almond orchards in Mediterranean regions face similar challenges, including hot, dry summers, increasing water scarcity, and the need for efficient irrigation practices (Fernandes de Oliveira et al., 2023; Medda et al., 2022). The RF model developed in this study incorporates key predictors such as air temperature, evaporation fraction, and vegetation indices, which are universally relevant under Mediterranean climatic conditions. However, regional variations, such as differences in soil types, almond cultivars, and irrigation practices, may influence SWP dynamics and model performance. Future research should explore the development of multiple models to estimate SWP using different sets of input variables, ranked by accuracy and uncertainty. This approach could provide practical tools for technicians and farmers with varying levels of data availability. While the current study focuses on presenting a robust and comprehensive model using the full set of available variables to maximize predictive accuracy, simplified models relying on fewer inputs could offer valuable alternatives. Developing, validating, and comparing such models would enable a systematic assessment of the trade-offs between data availability and model performance, offering tailored solutions for resource-constrained scenarios. In addition, future studies should investigate the influence of almond variety on irrigation requirements and water stress responses. Different almond varieties exhibit unique physiological traits, including root architecture, canopy structure, and drought tolerance, which can significantly impact water use efficiency and irrigation strategies. Incorporating varietal differences into predictive models could enhance the precision and applicability of irrigation recommendations. Further research could also focus on integrating additional environmental and biophysical factors, such as soil texture variability, salinity, and atmospheric conditions, to improve model robustness. Incorporating real-time remote sensing data from UAVs or satellites, combined with ground-based measurements, could enhance model scalability and accuracy. Testing these models under diverse climatic conditions and across different regions would further validate their transferability and practical utility.

5. Conclusion

This study demonstrates the significant potential of integrating high-resolution aerial imagery, satellite remote sensing, and meteorological data with advanced machine learning algorithms to improve the assessment of stem water potential (SWP) spatial variability in almond orchards. The Random Forest (RF) model developed in this research effectively predicts SWP, achieving high accuracy with an R^2 of up to 0.91 and a root mean square error (RMSE) of 0.17 MPa. The RF model's variable importance analysis identified air temperature, evaporation fraction, NDVI, and wind speed as the most significant predictors of SWP, reflecting their critical roles in tree water status. Additionally, 78.2 % of the model predictions fall within the "very good" category (NSE $\geq$ 0.90), confirming the model's high accuracy and reliability. The spatial maps generated by the RF model highlight substantial within-field variability in SWP, particularly during critical growth stages such as the hull split period. These maps provide valuable insights for precise irrigation management, enabling growers to identify areas experiencing greater water stress and adjust irrigation practices accordingly. This strategic approach helps mitigate water stress, thereby reducing the incidence of hull rot and ensuring better nut quality and yield. The integration of high-resolution remote sensing data and machine learning techniques offers a powerful tool for enhancing water management practices in almond orchards. Future research should focus on expanding these methodologies to other crops and regions and exploring incorporating additional environmental variables to refine prediction models further and enhance agricultural resilience to climatic variability.

CRediT authorship contribution statement

Srinivasa Rao Peddinti: Writing – original draft, Visualization, Methodology, Formal analysis, Data curation, Conceptualization. **Isaya Kisekka:** Writing – review & editing, Supervision, Project administration, Methodology, Funding acquisition, Formal analysis, Conceptualization.

Declaration of competing interest

The authors declare that they have no known competing financial interests or personal relationships that could have appeared to influence the work reported in this paper.

Acknowledgments

This study was supported by the USDA NIFA Award # 2021-68012-35914, and Almond Board of California Grant Project HORT69 Kisekka.

Data availability

Data will be made available on request.

References

Abrisqueta, I., Conejero, W., Valdés-Vela, M., Vera, J., Ortuño, M.F., Ruiz-Sánchez, M.C., 2015. Stem water potential estimation of drip-irrigated early-maturing peach trees under Mediterranean conditions. Comput. Electron. Agricult. 114, 7–13. https://doi.org/10.1016/j.compag.2015.03.004.

Arroyo, F.T., Herencia, J.F., Capote, N., 2022. Phenology, growth, and yield of almond cultivars under organic and conventional management in southwestern Spain. Span. J. Agricult. Res. 20, e0901. https://doi.org/10.5424/sjar/2022203-18828. –e0901.

Auret, L., Aldrich, C., 2012. Interpretation of nonlinear relationships between process variables by use of random forests. Miner. Eng. 35, 27–42. https://doi.org/10.1016/j.mineng.2012.05.008.

Awais, M., Li, W., Cheema, M.J.M., Zaman, Q.U., Shaheen, A., Aslam, B., Zhu, W., Ajmal, M., Faheem, M., Hussain, S., Nadeem, A.A., Afzal, M.M., Liu, C., 2023. UAV-based remote sensing in plant stress imagine using high-resolution thermal sensor for digital agriculture practices: a meta-review. Int. J. Environ. Sci. Technol. 20, 1135–1152. https://doi.org/10.1007/s13762-021-03801-5.

Badshah, A., Yousef Alkazemi, B., Din, F., Zamli, K.Z., Haris, M., 2024. Crop classification and yield prediction using robust machine learning models for agricultural sustainability. IEEE Access 12, 162799–162813. https://doi.org/10.1109/ACCESS.2024.3486653.

Bellvert, J., Adeline, K., Baram, S., Pierce, L., Sanden, B.L., Smart, D.R., 2018. Monitoring crop evapotranspiration and crop coefficients over an almond and pistachio orchard throughout remote sensing. Remote Sens. (Basel). https://doi.org/10.3390/rs10122001.

Bellvert, J., Nieto, H., Pelechá, A., Jofre-Čekalović, C., Zazurca, L., Miarnau, X., 2021. Remote sensing energy balance model for the assessment of crop evapotranspiration and water status in an almond rootstock collection. Front. Plant. Sci. 12, 288. https://doi.org/10.3389/fpls.2021.608967.

Beslic, Z., Pantelic, M., Dabic, D., Todic, S., Natic, M., Tesic, Z., 2015. Effect of vineyard floor management on water regime, growth response, yield and fruit quality in Cabernet Sauvignon. Sci. Hortic. 197, 650–656. https://doi.org/10.1016/j.scienta.2015.10.029.

Blum, A., 2011. Plant Water Relations, Plant Stress and Plant Production. In: Blum, A. (Ed.), Plant Breeding for Water-Limited Environments. Springer, New York, NY, pp. 11–52. https://doi.org/10.1007/978-1-4419-7491-4_2.

Calera, A., Campos, I., Osann, A., D'Urso, G., Menenti, M., 2017. Remote sensing for crop water management: from ET modelling to services for the end users. Sensors 17, 1104.

Choné, X., Van Leeuwen, C., Dubourdieu, D., Gaudillère, J.P., 2001. Stem water potential is a sensitive indicator of grapevine water status. Ann. Bot. 87, 477–483. https://doi.org/10.1006/anbo.2000.1361.

Cirhigiri, G.C., 2022. Qualitative Assessment of Windfall Almonds (Prunus dulcis) in California. University of California, Davis.

Datta, S., Taghvaeian, S., Ochsner, T.E., Moriasi, D., Gowda, P., Steiner, J.L., 2018. Performance assessment of five different soil moisture sensors under irrigated field conditions in Oklahoma. Sensor. (Switzerl.) 18, 3786. https://doi.org/10.3390/s18113786.

Domínguez-Niño, J.M., Oliver-Manera, J., Girona, J., Casadesús, J., 2020. Differential irrigation scheduling by an automated algorithm of water balance tuned by capacitance-type soil moisture sensors. Agricult. Water Manag. 228, 105880. https://doi.org/10.1016/j.agwat.2019.105880.

Drechsler, K., Fulton, A., Kisekka, I., 2022. Crop coefficients and water use of young almond orchards. Irrigat. Sci. 1, 1–17. https://doi.org/10.1007/s00271-022-00786-y.

Egea, G., González-Real, M.M., Baille, A., Nortes, P.A., Sánchez-Bel, P., Domingo, R., 2009. The effects of contrasted deficit irrigation strategies on the fruit growth and kernel quality of mature almond trees. Agricult. Water Manag. 96, 1605–1614. https://doi.org/10.1016/j.agwat.2009.06.017.

Egea, G., Nortes, P.A., González-Real, M.M., Baille, A., Domingo, R., 2010. Agronomic response and water productivity of almond trees under contrasted deficit irrigation regimes. Agricult. Water Manag. 97, 171–181. https://doi.org/10.1016/j.agwat.2009.09.006.

Fernandes de Oliveira, A., Mameli, M.G., De Pau, L., Satta, D., 2023. Almond tree adaptation to water stress: differences in physiological performance and yield responses among four cultivar grown in Mediterranean environment. Plants 12, 1131. https://doi.org/10.3390/plants12051131.

Fisher, J.B., Melton, F., Middleton, E., Hain, C., Anderson, M., Allen, R., McCabe, M.F., Hook, S., Baldocchi, D., Townsend, P.A., Kilic, A., Tu, K., Miralles, D.D., Perret, J., Lagouarde, J., Waliser, D., Purdy, A.J., French, A., Schimel, D., Famiglietti, J.S., Stephens, G., Wood, E.F., 2017. The future of evapotranspiration: global requirements for ecosystem functioning, carbon and climate feedbacks, agricultural management, and water resources. Water Resour. Res. 53, 2618–2626. https://doi.org/10.1002/2016WR020175.

Fulton, A., Grant, J., Buchner, R., Connell, J., 2014. Using the Pressure Chamber for Irrigation Management in Walnut, Almond and Prune. https://doi.org/10.3733/ucanr.8503.

Fulton, J., Norton, M., Shilling, F., 2019. Water-indexed benefits and impacts of California almonds. Ecol. Indic. 96, 711–717. https://doi.org/10.1016/j.ecolind.2017.12.063.

García-Tejero, I.F., Lipan, L., Gutiérrez-Gordillo, S., Durán Zuazo, V.H., Jančo, I., Hernández, F., Cárceles Rodríguez, B., Carbonell-Barrachina, Á.A., 2020. Deficit irrigation and its implications for HydroSOStainable almond production. Agronomy 10, 1632.

Garofalo, S.P., Giannico, V., Costanza, L., Alhajj Ali, S., Camposeo, S., Lopriore, G., Pedrero Salcedo, F., Vivaldi, G.A., 2024. Prediction of stem water potential in olive orchards using high-resolution planet satellite images and machine learning techniques. Agronomy 14, 1. https://doi.org/10.3390/agronomy14010001.

Goldhamer, D.A., Fereres, E., 2017. Establishing an almond water production function for California using long-term yield response to variable irrigation. Irrig. Sci. 35, 169–179. https://doi.org/10.1007/s00271-016-0528-2.

Goldhamer, D.A., Fereres, E., 2001. Simplified tree water status measurements can aid almond irrigation. Calif. Agric. (Berkeley) 55.

Goldhamer, D.A., Viveros, M., Salinas, M., 2006. Regulated deficit irrigation in almonds: effects of variations in applied water and stress timing on yield and yield components. Irrig. Sci. 24, 101–114. https://doi.org/10.1007/s00271-005-0014-8.

Gowda, P.H., Chavez, J.L., Colaizzi, P.D., Evett, S.R., Howell, T.A., Tolk, J.A., 2008. ET mapping for agricultural water management: present status and challenges. Irrig. Sci. 26, 223–237. https://doi.org/10.1007/s00271-007-0088-6.

Gutiérrez, S., Diago, M.P., Fernández-Novales, J., Tardaguila, J., 2018. Vineyard water status assessment using on-the-go thermal imaging and machine learning. PLoS ONE 13. https://doi.org/10.1371/journal.pone.0192037.

Gutiérrez-Gordillo, S., Lipan, L., Durán Zuazo, V.H., Sendra, E., Hernández, F., Hernández-Zazueta, M.S., Carbonell-Barrachina, Á.A., García-Tejero, I.F., 2020. Deficit irrigation as a suitable strategy to enhance the nutritional composition of hydrosos almonds. Water (Basel) 12, 3336.

Hedley, C.B., Yule, I.J., 2009. A method for spatial prediction of daily soil water status for precise irrigation scheduling. Agricult. Water Manag. 96, 1737–1745. https://doi.org/10.1016/j.agwat.2009.07.009.

Huang, B.F.F., Boutros, P.C., 2016. The parameter sensitivity of random forests. BMC Bioinform. 17, 331. https://doi.org/10.1186/s12859-016-1228-x.

Intrigliolo, D.S., Pérez, D., Risco, D., Yeves, A., Castel, J.R., 2012. Yield components and grape composition responses to seasonal water deficits in Tempranillo grapevines. Irrig. Sci. 30, 339–349. https://doi.org/10.1007/s00271-012-0354-0.

Irmak, S., Mutiibwa, D., 2010. On the dynamics of canopy resistance: generalized linear estimation and relationships with primary micrometeorological variables. Water Resour. Res. 46, 8526. https://doi.org/10.1029/2009WR008484.

Kim, D.W., Yun, H.S., Jeong, S.J., Kwon, Y.S., Kim, S.G., Lee, W.S., Kim, H.J., 2018. Modeling and testing of growth status for Chinese cabbage and white radish with UAV-based RGB imagery. Remote Sens. (Basel) 10, 563. https://doi.org/10.3390/rs10040563.

Kisekka, I., 2023. Orchard Water Management. In: Vougioukas, S.G., Zhang, Q. (Eds.), Advanced Automation for Tree Fruit Orchards and Vineyards. Springer International Publishing, Cham, pp. 59–74. https://doi.org/10.1007/978-3-031-26941-7_3.

Kisekka, I., Peddinti, S.R., Kustas, W.P., McElrone, A.J., Bambach-Ortiz, N., McKee, L., Bastiaanssen, W., 2022. Spatial–temporal modeling of root zone soil moisture dynamics in a vineyard using machine learning and remote sensing. Irrig. Sci. Under Rev.

Lambers, H., Oliveira, R.S., 2019. Plant Water Relations. In: Lambers, H., Oliveira, R.S. (Eds.), Plant Physiological Ecology. Springer International Publishing, Cham, pp. 187–263. https://doi.org/10.1007/978-3-030-29639-1_5.

Lin, Y., Zhu, Z., Guo, W., Sun, Y., Yang, X., Kovalskyy, V., 2020. Continuous monitoring of cotton stem water potential using Sentinel-2 imagery. Remote Sens. (Basel) 12, 1176. https://doi.org/10.3390/rs12071176.

Lipan, L., García-Tejero, I.F., Gutiérrez-Gordillo, S., Demirbaş, N., Sendra, E., Hernández, F., Durán-Zuazo, V.H., Carbonell-Barrachina, A.A., 2020. Enhancing nut quality parameters and sensory profiles in three almond cultivars by different irrigation regimes. J. Agric. Food Chem. 68, 2316–2328. https://doi.org/10.1021/acs.jafc.9b06854.

Ma, Y., Liu, S., Song, L., Xu, Z., Liu, Y., Xu, T., Zhu, Z., 2018. Estimation of daily evapotranspiration and irrigation water efficiency at a Landsat-like scale for an arid irrigation area using multi-source remote sensing data. Remote Sens. Environ. 216, 715–734. https://doi.org/10.1016/j.rse.2018.07.019.

Martí, P., Gasque, M., González-Altozano, P., 2013. An artificial neural network approach to the estimation of stem water potential from frequency domain reflectometry soil moisture measurements and meteorological data. Comput. Electron. Agricult. 91, 75–86. https://doi.org/10.1016/j.compag.2012.12.001.

Matese, A., Baraldi, R., Berton, A., Cesaraccio, C., Di Gennaro, S.F., Duce, P., Facini, O., Mameli, M.G., Piga, A., Zaldei, A., 2018. Estimation of Water Stress in grapevines using proximal and remote sensing methods. Remote Sens. (Basel) 10, 114. https://doi.org/10.3390/rs10010114.

Medda, S., Fadda, A., Mulas, M., 2022. Influence of climate change on metabolism and biological characteristics in perennial woody fruit crops in the mediterranean environment. Horticulturae 8, 273. https://doi.org/10.3390/horticulturae8040273.

Meyer, H., Reudenbach, C., Hengl, T., Katurji, M., Nauss, T., 2018. Improving performance of spatio-temporal machine learning models using forward feature selection and target-oriented validation. Environ. Modell. Softw. 101, 1–9. https://doi.org/10.1016/j.envsoft.2017.12.001.

Moriana, A., Pérez-López, D., Prieto, M.H., Ramírez-Santa-Pau, M., Pérez-Rodriguez, J.M., 2012. Midday stem water potential as a useful tool for estimating irrigation requirements in olive trees. Agricult. Water Manag. 112, 43–54. https://doi.org/10.1016/j.agwat.2012.06.003.

Olivo, N., Girona, J., Marsal, J., 2009. Seasonal sensitivity of stem water potential to vapour pressure deficit in grapevine. Irrig. Sci. 27, 175–182. https://doi.org/10.1007/s00271-008-0134-z.

O'Shaughnessy, S.A., Evett, S.R., Andrade, A., Workneh, F., Price, J.A., Rush, C.M., 2015. In: Site-specific variable rate irrigation as a means to enhance water use efficiencyJoint ASABE/IA Irrigation Symposium 2015: Emerging Technologies for Sustainable Irrigation. American Society of Agricultural and Biological Engineers, pp. 78–97. https://doi.org/10.13031/irrig.20152140448.

Otsu, N., 1979. A threshold selection method from gray-level histograms. IEEE Trans. Syst. Man Cybern. SMC-9, 62–66. https://doi.org/10.1109/tsmc.1979.4310076.

Parker, L., Pathak, T., Ostoja, S., 2021. Climate change reduces frost exposure for high-value California orchard crops. Sci. Total Environ. 762, 143971. https://doi.org/10.1016/j.scitotenv.2020.143971.

Peddinti, S.R., Hopmans, J.W., Najm, M.A., Kisekka, I., 2020. Assessing effects of salinity on the performance of a low-cost wireless soil water sensor. Sensor. (Switzerl.) 20, 1–14. https://doi.org/10.3390/s20247041.

Peddinti, S.R., Kambhammettu, B.P., 2019. Dynamics of crop coefficients for citrus orchards of central India using water balance and eddy covariance flux partition techniques. Agricult. Water Manag. 212. https://doi.org/10.1016/j.agwat.2018.08.027.

Peddinti, S.R., Kisekka, I., 2022. Estimation of turbulent fluxes over almond orchards using high-resolution aerial imagery with one and two-source energy balance models. Agricult. Water Manag. 269, 107671. https://doi.org/10.1016/J.AGWAT.2022.107671.

Peiris, P., Samanta, A., Mucchiani, C., Simons, C., Roy-Chowdhury, A., Karydis, K., et al., 2025. Vision-based xylem wetness classification in stem water potential determination. In: Bebis, G., Patel, V., Gu, J., Panetta, J., Gingold, Y., Johnsen, K., et al. (Eds.), Advances in Visual Computing. Springer Nature Switzerland, Cham, pp. 119–133. https://doi.org/10.1007/978-3-031-77389-1_10.

Pereira, L.S., Paredes, P., Jovanovic, N., 2020. Soil water balance models for determining crop water and irrigation requirements and irrigation scheduling focusing on the FAO56 method and the dual Kc approach. Agricult. Water Manag. 241, 106357. https://doi.org/10.1016/j.agwat.2020.106357.

Phinzi, K., Abriha, D., Szabó, S., 2021. Classification efficacy using k-fold cross-validation and bootstrapping resampling techniques on the example of mapping complex gully systems. Remote Sens. (Basel) 13, 2980. https://doi.org/10.3390/rs13152980.

Poblete, T., Ortega-Farías, S., Moreno, M.A., Bardeen, M., 2017. Artificial Neural Network to Predict Vine Water Status Spatial Variability Using Multispectral Information Obtained from an Unmanned Aerial Vehicle (UAV). Sens. (Basel) 17. https://doi.org/10.3390/S17112488.

Politis, D.N., Romano, J.P., 1994. Large sample confidence regions based on subsamples under minimal assumptions. Ann. Statist. 22, 2031–2050.

Rashid, M., Bari, B.S., Yusup, Y., Kamaruddin, M.A., Khan, N., 2021. A Comprehensive Review of Crop Yield Prediction Using Machine Learning Approaches With Special Emphasis on Palm Oil Yield Prediction. IEEE Access 9, 63406–63439. https://doi.org/10.1109/ACCESS.2021.3075159.

Ritter, A., Muñoz-Carpena, R., 2013. Performance evaluation of hydrological models: statistical significance for reducing subjectivity in goodness-of-fit assessments. J. Hydrol. 480, 33–45. https://doi.org/10.1016/j.jhydrol.2012.12.004.

Rodriguez-Galiano, V., Sanchez-Castillo, M., Chica-Olmo, M., Chica-Rivas, M., 2015. Machine learning predictive models for mineral prospectivity: an evaluation of

neural networks, random forest, regression trees and support vector machines. Ore Geol. Rev. 71, 804–818. https://doi.org/10.1016/j.oregeorev.2015.01.001.
Romero, M., Luo, Y., Su, B., Fuentes, S., 2018. Vineyard water status estimation using multispectral imagery from an UAV platform and machine learning algorithms for irrigation scheduling management. Comput. Electron. Agricult. 147, 109–117. https://doi.org/10.1016/j.compag.2018.02.013.
Irmak, S., Mutiibwa, D., 2009. On the dynamics of stomatal resistance: relationships between stomatal behavior and micrometeorological variables and performance of Jarvis-type parameterization. Transact. ASABE 52, 1923–1939. https://doi.org/10.13031/2013.29219.
Sarvakar, K., Thakkar, M., 2024. Different vegetation indices measurement using computer vision. In: Chouhan, S.S., Singh, U.P., Jain, S. (Eds.), Applications of Computer Vision and Drone Technology in Agriculture 4.0. Springer Nature, Singapore, pp. 133–163. https://doi.org/10.1007/978-981-99-8684-2_9.
Savchik, P., Nocco, M., Kisekka, I., 2024. Mapping almond stem water potential using machine learning and multispectral imagery. Irrig. Sci. https://doi.org/10.1007/s00271-024-00932-8.
Seyar, M.H., Ahamed, T., 2024. Optimization of soil-based irrigation scheduling through the integration of machine learning, remote sensing, and soil moisture sensor technology. In: Ahamed, T. (Ed.), IoT and AI in Agriculture: Smart Automation Systems for Increasing Agricultural Productivity to Achieve SDGs and Society 5.0. Springer Nature, Singapore, pp. 275–299. https://doi.org/10.1007/978-981-97-1263-2_18.
Shackel, K., Moriana, A., Marino, G., Corell, M., Pérez-López, D., Martin-Palomo, M.J., Caruso, T., Marra, F.P., Agüero Alcaras, L.M., Milliron, L., Rosecrance, R., Fulton, A., Searles, P., 2021. Establishing a reference baseline for midday stem water potential in olive and its use for plant-based irrigation management. Front. Plant. Sci. 12, 2715. https://doi.org/10.3389/fpls.2021.791711.
Shanley, C.S., Eacker, D.R., Reynolds, C.P., Bennetsen, B.M.B., Gilbert, S.L., 2021. Using LiDAR and random forest to improve deer habitat models in a managed forest landscape. For. Ecol. Manage. 499, 119580. https://doi.org/10.1016/j.foreco.2021.119580.
Sharma, K., Irmak, S., Kukal, M.S., 2021. Propagation of soil moisture sensing uncertainty into estimation of total soil water, evapotranspiration and irrigation decision-making. Agricult. Water Manag. 243, 106454. https://doi.org/10.1016/j.agwat.2020.106454.
Smith, E., 2021. Early Almond Harvest As a Sustainable Pest Management Strategy. University of California, Davis.
Smith, E.E., Brown, P.H., Andrews, E.M., Shackel, K.A., Holtz, B.A., Rivers, D.J., Haviland, D.R., Khalsa, S.D.S., 2022. Early almond harvest as a strategy for sustainable irrigation, pest and disease management. Sci. Hortic. 293, 110651. https://doi.org/10.1016/j.scienta.2021.110651.
Soulis, K.X., Elmaloglou, S., Dercas, N., 2015. Investigating the effects of soil moisture sensors positioning and accuracy on soil moisture based drip irrigation scheduling systems. Agricult. Water Manag. 148, 258–268. https://doi.org/10.1016/j.agwat.2014.10.015.
Stewart, W.L., Fulton, A.E., Krueger, W.H., Lampinen, B.D., Shackel, K.A., 2011. Regulated deficit irrigation reduces water use of almonds without affecting yield. Calif. Agric. (Berkeley) 65.
Valente, A., Costa, C., Pereira, L., Soares, B., Lima, J., Soares, S., 2022. A LoRaWAN IoT system for smart agriculture for vine water status determination. Agriculture 12, 1695. https://doi.org/10.3390/agriculture12101695.
Van Beek, J., Tits, L., Somers, B., Coppin, P., 2013. Stem Water Potential Monitoring in Pear Orchards through worldview-2 Multispectral Imagery. Remote Sens. (Basel) 5, 6647–6666. https://doi.org/10.3390/rs5126647.
Vuppalapati, C., 2023. Specialty crops almonds. In: Vuppalapati, C. (Ed.), Specialty Crops for Climate Change Adaptation: Strategies for Enhanced Food Security by Using Machine Learning and Artificial Intelligence. Springer Nature Switzerland, Cham, pp. 627–741. https://doi.org/10.1007/978-3-031-38399-1_7.
Xu, C.-Y., Singh, V.P., 1998. A review on monthly water balance models for water resources investigations. Water Resour. Manag. 12, 20–50.
Yada, S., Huang, G., Lapsley, K., 2013. Natural variability in the nutrient composition of California-grown almonds. J. Food Compos. Analy. 30, 80–85. https://doi.org/10.1016/j.jfca.2013.01.008.
Yang, Y., Anderson, M., Gao, F., Xue, J., Knipper, K., Hain, C., 2022. Improved daily evapotranspiration estimation using remotely sensed data in a data fusion system. Remote Sens. (Basel) 14, 1772. https://doi.org/10.3390/rs14081772.
Zhao, T., Chen, Y.Q., Ray, A., Doll, D., 2017a. Quantifying almond water stress using unmanned aerial vehicles (UAVS): correlation of stem water potential and higher order moments of non-normalized canopy distribution. In: Proceedings of the ASME Design Engineering Technical Conference. https://doi.org/10.1115/DETC2017-68246.
Zhao, T., Stark, B., Chen, Y., Ray, A.L., Doll, D., 2015. A detailed field study of direct correlations between ground truth crop water stress and normalized difference vegetation index (NDVI) from small unmanned aerial system (sUAS). In: 2015 International Conference on Unmanned Aircraft Systems, ICUAS 2015. Institute of Electrical and Electronics Engineers Inc., pp. 520–525. https://doi.org/10.1109/ICUAS.2015.7152331
Zhao, T., Stark, B., Chen, Y.Q., Ray, A.L., Doll, D., 2017b. Challenges in water stress quantification using small unmanned aerial system (sUAS): lessons from a growing season of almond. J. Intell. Robot. Syst.: Theory Applic. 88, 721–735. https://doi.org/10.1007/s10846-017-0513-x.